Distributed Deployment Algorithms for Improved Coverage in a Network of Wireless Mobile Sensors

Hamid Mahboubi, *Member, IEEE*, Kaveh Moezzi, *Member, IEEE*, Amir G. Aghdam, *Senior Member, IEEE*, Kamran Sayrafian-Pour, *Senior Member, IEEE*, and Vladimir Marbukh, *Senior Member, IEEE*

***Abstract*—In this paper, efficient sensor deployment strategies are developed to increase coverage in wireless mobile sensor networks. The sensors find coverage holes within their Voronoi polygons and then move in an appropriate direction to minimize them. Novel edge-based and vertex-based strategies are introduced, and their performances are compared with existing techniques. The proposed movement strategies are based on the distances of each sensor and the points inside its Voronoi polygon from the edges or vertices of the polygon. Simulations confirm the effectiveness of the proposed deployment algorithms and their superiority to the techniques reported in the literature.**

***Index Terms*—Coverage, mobile sensors, wireless sensor networks.**

I. Introduction

WIRELESS sensor networks have attracted considerable attention in various research communities in recent years, due to their widespread applications [1]–[4]. Such applications range from biomedical engineering to rescue missions to target tracking and surveillance [5]–[8]. Researchers in diverse disciplines have made significant contributions to the field by developing mathematical models for the operation of the system [9], designing cost-effective resource management techniques for prolonging network lifetime [10], [11], and deriving efficient deployment algorithms to increase the coverage of the network [12], [13].

Coverage improvement is a typical goal of a mobile sensor network. In this type of problem, it is desired to move a group of sensors and place them in appropriate locations in order to monitor the environment more effectively. There is often no *a priori* knowledge of the environment and the initial positions of the sensors [14]. Furthermore, due to the distributed nature of the network, it is more desirable to minimize the information exchange between the sensors. In fact, each sensor has limited communication and sensing ranges, and it is not feasible for the sensors to communicate with a central server in order to obtain information about the entire network [15], [16].

In [17], location services (which are concerned with obtaining the position information of the destination) for mobile *ad-hoc* networks are reviewed. A new coverage model called surface coverage is proposed in [18], and two important problems are studied: 1) expected coverage ratio with stochastic deployment and 2) optimal deployment strategy with planned deployment. In [19], distributed control laws are presented to achieve a convex equipartition configuration in mobile sensor networks. Distributed control laws are provided in [20] for the disk-covering and sphere-packing problems using nonsmooth gradient flows. An algorithm is proposed in [21] for environmental boundary tracking with mobile agents, where the boundary is optimally approximated with a polygon. In [22], an approach is presented for energy-efficient coverage in wireless sensor networks using an ant colony optimization algorithm.

The basic protocol approach is proposed in [23], where the sensors find their final destination using an iterative procedure. An alternative technique, namely virtual movement protocol, is proposed in [13] which does not require the sensors to move physically unless the communication cost is too high or the final destinations are determined. Three distributed self-deployment algorithms are subsequently proposed to determine the final destination of the sensors: 1) VOR (Voronoi-based algorithm); 2) VEC (vector-based algorithm); and 3) Minimax [13]. In the VOR algorithm, the distance of each sensor from the vertices of its Voronoi polygon is obtained, and the desired location for the sensor is calculated accordingly. The VEC algorithm, on the other hand, is a "proactive" strategy under which the sensors are relocated to achieve an even distribution in the sensing field. In the Minimax algorithm, each sensor moves (more smoothly compared with other algorithms) to a point inside its Voronoi polygon such that its maximum distance from the vertices of the polygon is the smallest. While the above techniques are effective in terms of coverage, they suffer from a number of shortcomings. For example, in the VOR and Minimax approaches, if a sensor is located close to a narrow edge in its Voronoi polygon, it does not need to move much, and, as a consequence, the coverage holes may not be reduced. Furthermore, sensing coverage achieved by the VEC algorithm may not be satisfactory compared with other methods, when there is a relatively large number of sensors in the network.

Manuscript received February 02, 2012; revised August 15, 2012, November 22, 2012, and January 31, 2013; accepted March 15, 2013. Date of publication September 04, 2013; date of current version December 12, 2014. This work was supported by the National Institute of Standards and Technology (NIST) under Grant 70NANB8H8146. Paper no. TII-12-0051.

H. Mahboubi and A. G. Aghdam are with the Department of Electrical and Computer Engineering, Concordia University, Montréal, QC H3G 1M8 Canada (e-mail: h_mahbo@ece.concordia.ca; aghdam@ece.concordia.ca).

K. Moezzi is with Bombardier, Montréal, QC H3B 1X9 Canada (e-mail: kaveh.moezzi@aero.bombardier.com).

K. Sayrafian-Pour and V. Marbukh are with the National Institute of Standards and Technology (NIST), Gaithersburg, MD 20899 USA (e-mail: ksayrafian@nist.gov; marbukh@nist.gov).

Color versions of one or more of the figures in this paper are available online at http://ieeexplore.ieee.org.

Digital Object Identifier 10.1109/TII.2013.2280095

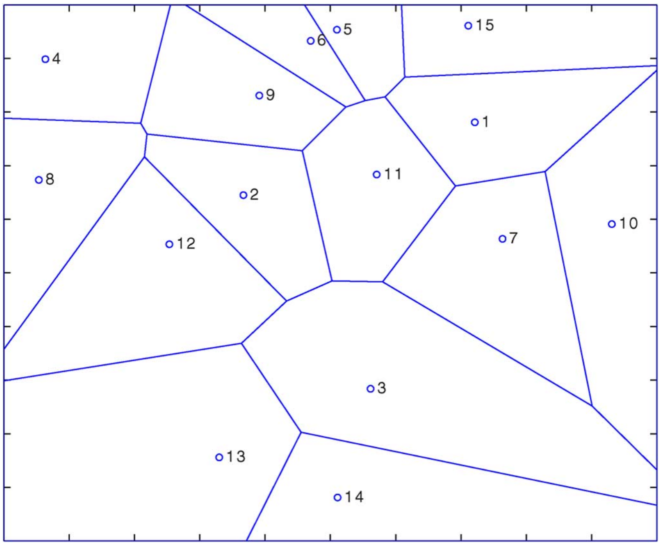

Fig. 1. Example of a Voronoi diagram.

In this paper, four new techniques are introduced to increase coverage in a mobile sensor network. The Maxmin-vertex and Maxmin-edge algorithms tend to maximize the minimum distance of every sensor from the vertices and edges, respectively, of its Voronoi polygon. The Minimax-edge algorithm, on the other hand, tends to minimize the maximum distance of every sensor from the edges of its Voronoi polygon. Finally, the VEDGE algorithm is a combination of the Maxmin-edge algorithm (as an edge-based technique) and the Minimax algorithm (as a vertex-based technique). The main characteristic of these algorithms is that the sensor movement is performed iteratively, and the coverage is guaranteed to increase after each iteration. The proposed techniques are evaluated by simulation in terms of coverage performance, convergence rate, and energy-efficiency. The suitability of each technique for different scenarios is discussed.

This paper is organized as follows. In Section II, preliminary material concerning the Voronoi diagram is provided and its properties are briefly discussed. Section III presents the proposed algorithms for efficient coverage, as the main contribution of the paper. In Section IV, simulation results are given to show the effectiveness of the proposed approaches. Finally, concluding remarks are drawn in Section V.

II. Preliminaries

Consider a flat polygon-shaped surface and a set of networked sensors denoted by $\mathbf{S} := \{S_1, S_2, \ldots, S_n\}$. Let the network be represented by a graph, where each node denotes a sensor. Partition the plane into n convex polygons such that each polygon contains only one node, called the generating node of that polygon, and any point inside each polygon is closer to its generating node than to any other node in the plane. The resultant diagram is called a Voronoi diagram, and each individual cell in it is referred to as a Voronoi polygon (or region). An example of a Voronoi diagram for a network of 15 sensors is depicted in Fig. 1.

The Voronoi region Π_i generated by S_i can be mathematically formulated as (see [24] and [25])

$$\Pi_i = \left\{X \in \mathbb{R}^2 | d(X, Y_i) \leq d(X, Y_j), j \in \mathbf{n} := \{1, \ldots, n\}, i \neq j\right\} \tag{1}$$

where Y_i is the coordinate of S_i, and $d(X, Y_i)$ denotes the Euclidean distance between the points X and Y_i in the 2-D plane. To construct the Voronoi diagram, the bisectors of each node and its neighbors need to be drawn first. Among all polygons generated by these bisectors, the smallest one which contains the node is the Voronoi polygon of that node. It follows from (1) that any point in a Voronoi polygon which is not detected by the sensor associated with that polygon cannot be detected by any other sensor either. Thus, in order to find the so-called "coverage holes," i.e., the points that are not detected by any sensor in the network, each sensor would only need to check its own Voronoi polygon. The Voronoi diagram is used for the analysis and synthesis of sensor deployment algorithms in this paper.

Definition 1: A pair of nodes whose Voronoi polygons share an edge are referred to as *neighbors*.

Definition 2: Consider a sensor S_i with the sensing radius r and the corresponding Voronoi polygon $\Pi_i, i \in \mathbf{n}$, and let Q be an arbitrary point inside Π_i. The intersection of the polygon Π_i and a circle of radius r centered at Q is referred to as the ith *coverage area w.r.t.* Q, and is denoted by $\beta^Q_{\Pi_i}$. The ith coverage area w.r.t. the location of the sensor S_i is called the *local coverage area* of that sensor [26].

Definition 3: Consider an arbitrary point Q inside the Voronoi polygon Π_i, $i \in \mathbf{n}$. The area inside the Voronoi polygon Π_i which lies outside the ith coverage area w.r.t. Q is referred to as the ith *coverage hole w.r.t.* Q and is denoted by $\theta^Q_{\Pi_i}$. The ith coverage hole w.r.t. the location of the sensor S_i is called the *local coverage hole* of that sensor. Also, the union of all local coverage holes in the sensing field is referred to as the *total coverage hole*, and is denoted by θ, i.e., $\theta = \sum_{i=1}^{n} \theta^{P_i}_{\Pi_i}$, where P_i denotes the location of the sensor S_i.

Assumption 1: In this paper, it is assumed that there is no obstacle in the field. This means that every sensor can move to any desired location using existing techniques, e.g., the ones provided in [13], [23], [27], and [28].

Assumption 2: All sensors are assumed to be capable of locating themselves in the field (using, for instance, the methods proposed in [29] and [30]). Moreover, the localization error of every sensor is assumed to be negligible [13], [28].

Assumption 3: It is assumed that the graph representing sensors' communication topology is connected [31]. Hence, each sensor can obtain the information about the locations of the other sensors through proper communication routes, and consequently calculate its Voronoi polygon accurately (using the position information of its neighbors). Note that this is a realistic assumption as the number of sensors in a mobile sensor network is typically large (or, more precisely, there is a sufficient number of sensors per area unit) [32], [33].

Problem Statement: In this work, it is desired that each sensor finds a candidate location for itself using the available local information and moves to this new position such that the total coverage of the network increases (or, equivalently, the total coverage hole decreases).

III. Main Results

Here, four efficient sensor relocation algorithms are introduced to increase sensing coverage in a mobile sensor network. The main characteristic of these algorithms is that the sensor movement is performed iteratively until the termination condition is satisfied. Each round in the proposed algorithms consists of four phases. In the first phase, every sensor S_i, $i \in \mathbf{n}$, broadcasts its location information to other sensors and then constructs its Voronoi polygon based on the similar information it receives from other sensors. Then, in the second phase, each sensor checks its polygon for possible coverage holes. If any coverage hole exists, the sensor finds a candidate location $\acute{P}_i$ for itself (but does not move there) using an appropriate scheme, such that by moving there the coverage hole would be eliminated, or at least its size would be reduced by a certain threshold. Once the new candidate location is calculated, the coverage area w.r.t. this location, i.e., $\beta_{\Pi_i}^{\acute{P}_i}$, is obtained in the third phase. If this coverage area is greater than the current local coverage area, i.e. $\beta_{\Pi_i}^{\acute{P}_i} > \beta_{\Pi_i}^{P_i}$, the sensor moves to the new destination; otherwise, it remains at its current location. Finally, in the termination phase, if none of the sensors' local coverage area in its Voronoi polygon would be increased by a certain amount, the iterations stop. This termination condition guarantees that the proposed algorithms stop in finite time.

As noted above, one of the important characteristics of the sensor deployment strategies proposed in this paper is that each sensor moves to a new location only if its coverage area w.r.t. the new location in the old Voronoi polygon increases. Similar to Theorem 1 of [26], it is shown below that, under this type of deployment scheme, the total coverage increases.

Theorem 1: Consider the set $\mathbf{S}$ of n sensors described in the previous section, and let the position of the ith sensor be denoted by P_i, with the corresponding Voronoi polygon Π_i. Assume the ith sensor moves to a new position $\acute{P}_i$, for any $i \in \mathbf{n}$, with the corresponding Voronoi polygon $\acute{\Pi}_i$ such that $\acute{P}_i \neq P_i$ if and only if $i \in \mathbf{k}$, where $\mathbf{k}$ is a non-empty subset of $\mathbf{n}$. If the i-th coverage area w.r.t. $\acute{P}_i$ in the previously constructed Voronoi polygon Π_i is greater than the ith local coverage area in Π_i (i.e., $\beta_{\Pi_i}^{\acute{P}_i} > \beta_{\Pi_i}^{P_i}$) for all $i \in \mathbf{k}$, then the total coverage in the network increases.

Proof: Let the total uncovered area of the sensing field when the sensors are located at the positions $\mathbf{P} = \{P_1, P_2, \ldots, P_n\}$ and $\acute{\mathbf{P}} = \{\acute{P}_1, \acute{P}_2, \ldots, \acute{P}_n\}$ be denoted by θ and $\acute{\theta}$, respectively. From the characterization of the Voronoi diagram, one can write

$$\theta = \sum_{i=1}^{n} \theta_{\Pi_i}^{P_i}. \tag{2}$$

It is straightforward to show that for any $i \in \mathbf{k}$, if the coverage area in Π_i increases, then the corresponding coverage hole will become smaller. Since it is assumed that the ith coverage area w.r.t. $\acute{P}_i$ is greater than the ith local coverage area for any $i \in \mathbf{k}$, one can conclude that

$$\theta_{\Pi_i}^{\acute{P}_i} < \theta_{\Pi_i}^{P_i} \quad \forall i \in \mathbf{k}. \tag{3}$$

In addition, note that, if $\acute{P}_i = P_i$, then

$$\theta_{\Pi_i}^{\acute{P}_i} = \theta_{\Pi_i}^{P_i} \quad \forall i \in \mathbf{n} \setminus \mathbf{k}. \tag{4}$$

On the other hand, it is possible that part of the area in $\theta_{\Pi_i}^{\acute{P}_i}$ is also covered by some other sensors in the set $\mathbf{n} \setminus \{i\}$. Hence

$$\acute{\theta} \leq \sum_{i=1}^{n} \theta_{\Pi_i}^{\acute{P}_i}. \tag{5}$$

Furthermore, from (3), (4), and (5), one arrives at the following inequality:

$$\acute{\theta} < \sum_{i=1}^{n} \theta_{\Pi_i}^{P_i}. \tag{6}$$

Now, it is concluded from (2) and (6) that

$$\acute{\theta} < \theta \tag{7}$$

which means that the total coverage area increases using the proposed deployment scheme. ■

A. Maxmin-Vertex Strategy

The rationale behind the Maxmin-vertex strategy is that, when the sensors are evenly distributed, none of them should be too close to any of its Voronoi vertices. In this strategy, a point inside the Voronoi polygon whose distance from the nearest Voronoi vertex is the largest is selected as the candidate destination point. This point will be referred to as the *Maxmin-vertex centroid* and will be denoted by $\bar{O}$. Let the distance between this point and the nearest vertex to it on the polygon be represented by $\bar{r}$. Also, let $C(O, r)$ denote a circle of radius r centered at the point O. The Maxmin-vertex circle is defined next.

Definition 4: The Maxmin-vertex circle of a polygon is defined as the largest circle centered inside the polygon such that all of the vertices of the polygon are either outside the circle, or on it. This circle is, in fact, $C(\bar{O}, \bar{r})$.

Lemma 1: The Maxmin-vertex circle passes through at least two Voronoi vertices.

Proof: Let $\bar{V}$ be the nearest vertex of the ith polygon to its Maxmin-vertex centroid $\bar{O}$, and define

$$\hat{u} := \min_{V \in \mathbf{V}_i - \{\bar{V}\}} \left\{ d(\bar{O}, V) \right\}, \quad i \in \mathbf{n} \tag{8}$$

where $\mathbf{V}_i$ is the set of all vertices of polygon i in the Voronoi diagram. Suppose that the Maxmin-vertex circle does not pass through any vertex other than $\bar{V}$, and hence $\delta^* = (\hat{u} - \bar{r})/2$ is positive. There are two possibilities, as discussed below.

Case 1) $\bar{O}$ *is inside the polygon*. Let $\hat{O}$ be a point on the line $\bar{V}\bar{O}$, but closer to $\bar{O}$, such that the distance between

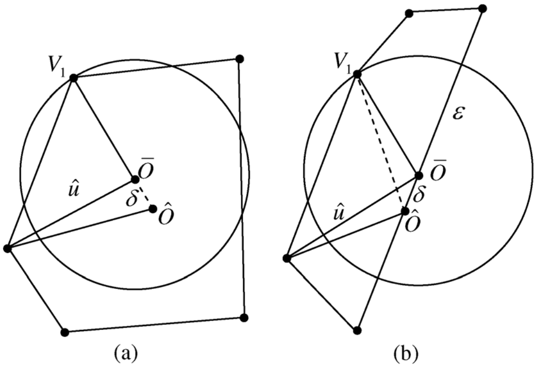

Fig. 2. Diagram of a Voronoi polygon and the corresponding Maxmin-vertex circle when the Maxmin-vertex centroid is (a) inside the polygon and (b) on the polygon.

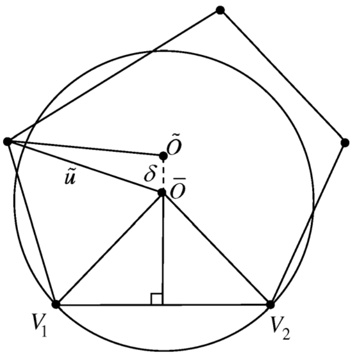

Fig. 3. Diagram used in the proof of Lemma 2.

$\bar{O}$ and $\hat{O}$ is equal to δ, where δ is an arbitrary value in $(0, \delta^*]$ [see Fig. 2(a)].

Case 2) *$\bar{O}$ is on the polygon*. Suppose $\bar{O}$ is on the edge ε. Let $\hat{O}$ be a point on ε such that $d(\hat{O}, \bar{V}) > d(\bar{O}, \bar{V})$ and the distance between $\bar{O}$ and $\hat{O}$ is equal to δ, where δ is an arbitrary value in the interval $(0, \delta^*]$ [see Fig. 2(b)].

In both cases, according to the triangle inequality, we have

$$d(\hat{O}, V) \geq d(\bar{O}, V) - \delta \geq \hat{u} - \delta, \quad \forall V \in \mathbf{V}_i - \{\bar{V}\}, \quad i \in \mathbf{n}. \tag{9}$$

From the above relation and noting that $\hat{u} - \delta \geq \bar{r} + \delta > \bar{r}$, it can be concluded that

$$\min_{V \in \mathbf{V}_i} \left\{ d(\hat{O}, V) \right\} > \bar{r} \tag{10}$$

which contradicts the fact that $\bar{O}$ is the Maxmin-vertex centroid. Thus, there is at least one more vertex on the Maxmin-vertex circle, and this completes the proof. ■

Lemma 2: If the Maxmin-vertex circle passes through exactly two Voronoi vertices, say $\bar{V}_1$ and $\bar{V}_2$, then $\bar{O}$ is the intersection of the perpendicular bisector of $\bar{V}_1\bar{V}_2$ and an edge of the polygon.

Proof: Suppose $\bar{O}$ is not the intersection of the perpendicular bisector of $\bar{V}_1\bar{V}_2$ and an edge of the polygon, i.e., $\bar{O}$ is inside the polygon. Define

$$\tilde{u} := \min_{V \in \mathbf{V}_i - \{\bar{V}_1, \bar{V}_2\}} \left\{ d(\bar{O}, V) \right\}, \quad i \in \mathbf{n}. \tag{11}$$

Since $C(\bar{O}, \bar{r})$ passes through exactly two vertices, thus $\delta^* = (\tilde{u} - \bar{r})/2$ is positive. Let $\tilde{O}$ be a point on the perpendicular bisector of $\bar{V}_1\bar{V}_2$ and outside the triangle $\bar{V}_1\bar{V}_2\bar{O}$, but closer to $\bar{O}$, such that the distance between the points $\bar{O}$ and $\tilde{O}$ is equal to δ, where δ is an arbitrary value in the interval $(0, \delta^*]$ (see Fig. 3). Using the triangle inequality, one can write

$$d(\tilde{O}, V) \geq d(\bar{O}, V) - \delta \geq \tilde{u} - \delta. \tag{12}$$

The above result along with the relations $\tilde{u} - \delta \geq \tilde{u} - \delta^* = \bar{r} + \delta^* > \bar{r}$ and $d(\tilde{O}, \bar{V}_1) = d(\tilde{O}, \bar{V}_2) > \bar{r}$ yields

$$\min_{V \in \mathbf{V}_i} \left\{ d(\tilde{O}, V) \right\} > \bar{r}, \quad i \in \mathbf{n} \tag{13}$$

which contradicts the fact that $\bar{O}$ is the Maxmin-vertex centroid. ■

Definition 5: For convenience of notation, the circle passing through two vertices V_p and V_q of polygon i, centered at the intersection of the perpendicular bisector of V_pV_q and the edge V_kV_l, is denoted by $\Omega^{k,l}_{p,q}$, $k, l, p, q \in \mathbf{m}_i := \{1, \ldots, m_i\}$, where m_i is the number of vertices of the ith polygon, for any $i \in \mathbf{n}$. Also, the circle passing through three vertices V_p, V_q and V_r of polygon i is denoted by $\Omega_{p,q,r}$, for $p, q, r \in \mathbf{m}_i$.

Theorem 2: For any $k, l, p, q \in \mathbf{m}_i$, let $\breve{\mathbf{C}}_i$ be the set of all circles $\Omega^{k,l}_{p,q}$ whose centers are on polygon i, and do not enclose any of the vertices of the polygon, and $\grave{\mathbf{C}}_i$ be the set of all circumcircles of any three vertices, centered inside or on the polygon, which do not enclose any of the vertices of the polygon. Define $\mathbf{C}_i := \breve{\mathbf{C}}_i \cup \grave{\mathbf{C}}_i$. Then, $C(\bar{O}, \bar{r}) \in \mathbf{C}_i$, and also for all $C(O, r) \in \mathbf{C}_i, r \leq \bar{r}$.

Proof: According to Lemma 1, the Maxmin-vertex circle passes through at least two Voronoi vertices. If it passes through exactly two Voronoi vertices, say V_1 and V_2, then according to Lemma 2 there exist $k, l \in \mathbf{m}_i$ such that $C(\bar{O}, \bar{r}) = \Omega^{k,l}_{1,2}$. Hence, in this case, $C(\bar{O}, \bar{r}) \in \mathbf{C}_i$, and, from Definition 4, $\bar{r} = \max_{C(O,r) \in \mathbf{C}_i} \{r\}$. If, on the other hand, the Maxmin-vertex circle passes through three or more Voronoi vertices, then it is the circumcircle of those vertices. Therefore, $C(\bar{O}, \bar{r}) \in \mathbf{C}_i$, and again it is deduced from Definition 4 that $\bar{r} = \max_{C(O,r) \in \mathbf{C}_i} \{r\}$. ■

Using the result of Theorem 2, one can develop an algorithm of complexity $O(m_i^4)$ to calculate the Maxmin-vertex centroid in Voronoi polygon i. Since typically a Voronoi polygon does not have too many vertices, the computational complexity of such an algorithm is not expected to be high, typically. Detailed steps are presented in Algorithm 1.

The sensor deployment technique discussed above as well as the two algorithms given in [13] are all vertex-based, in the sense that they are concerned with the distances of the nodes from the vertices of the Voronoi diagram. While algorithms of this type prove effective in many cases, they may not be as effective for certain node configurations. For instance, consider the polygon in Fig. 4, and let the sensor be placed at point S. It is easy to verify that in order to increase the coverage area, the sensor must move to the left. However, both VOR and Minimax algorithms proposed in [13] consider the candidate points A and B, respectively, which are in the right side of S. To

Algorithm 1: Finding the Maxmin-vertex centroid of the i-th Voronoi polygon

```
begin
  1) for $p = 1, 2, \ldots, m_i - 2$
       for $q = p+1, p+2, \ldots, m_i - 1$
         for $r = q+1, q+2, \ldots, m_i$
           calculate $\Omega_{p,q,r}$
           if $\Omega_{p,q,r}$ is centered inside or on the
           polygon and does not enclose any of the
           vertices of the polygon, then
               record it.
           end
         end
       end
     end
  2) for $p = 1, 2, \ldots, m_i - 1$
       for $q = p+1, p+2, \ldots, m_i$
         calculate $\Omega^{k,l}_{p,q}$
         if $\Omega^{k,l}_{p,q}$ is centered on the polygon and
         does not enclose any of the vertices of the
         polygon, then
             record it.
         end
       end
     end
  3) The center of the largest circle is the
     Maxmin-vertex centroid of the polygon.
```

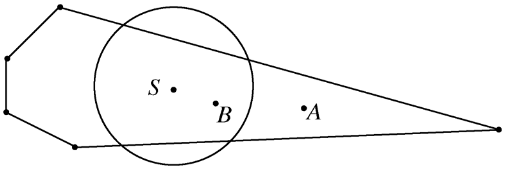

Fig. 4. Example of a configuration for which the vertex-based strategies are not as effective.

remedy this shortcoming of the vertex-based algorithms, two edge-based techniques will be presented in Section III-B.

B. Minmax-Edge Strategy

The rationale behind the Minmax-edge technique is that when the sensors are evenly distributed, none of them should be too far from any of its Voronoi edges. The Minmax-edge strategy chooses the candidate location of the sensor S_i as a point inside Voronoi polygon i whose distance from the farthest Voronoi edge is the smallest. This point will be referred to as the *Minmax-edge centroid*, and will be denoted by $\acute{O}$. Furthermore, the distance between this point and the farthest edge on Voronoi polygon i will be represented by $\acute{r}$. In the remainder of this subsection, intersecting or tangent to or touching an edge means intersecting or tangent to or touching that edge or its extension. The Minmax-edge circle is defined next.

Definition 6: The Minmax-edge circle is the smallest circle centered inside or on a polygon, intersecting or touching all of its edges. This circle is in fact $C(\acute{O}, \acute{r})$ and is not necessarily unique (this issue will be addressed later).

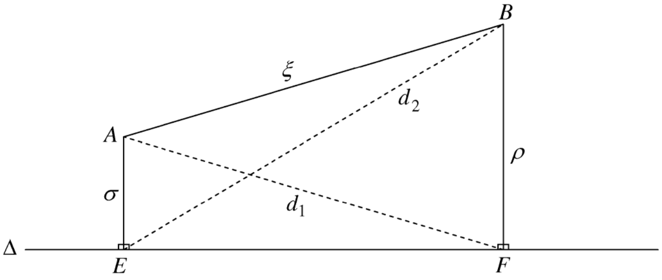

Fig. 5. Diagram used in the proof of Lemma 3.

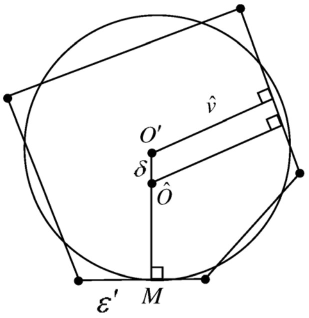

Fig. 6. Diagram used in the proof of Lemma 4.

Lemma 3: Consider two points A, B and a line Δ. Let the distance between A and Δ be denoted by σ, and that between B and Δ by ρ. Let also the length of the segment AB be denoted by ξ. Then

$$\sigma - \xi \le \rho \le \sigma + \xi. \tag{14}$$

Proof: Let E and F be two points on Δ, such that $AE \perp \Delta$ and $BF \perp \Delta$. Let $d(A, F) = d_1$ and $d(B, E) = d_2$ (see Fig. 5). According to the triangle inequality

$$\sigma \le d_1 \le \rho + \xi \tag{15}$$
$$\rho \le d_2 \le \sigma + \xi. \tag{16}$$

Relation (14) follows directly from (15) and (16). ■

Lemma 4: The Minmax-edge circle is tangent to at least two of the edges of its Voronoi polygon.

Proof: Let $\acute{\varepsilon}$ be the farthest edge from the Minmax-edge centroid of a given Voronoi polygon. It is obvious that $\acute{r}$ is equal to the distance between $\acute{O}$ and $\acute{\varepsilon}$, denoted by $d(\acute{O}, \acute{\varepsilon})$. Thus, $C(\acute{O}, \acute{r})$ is tangent to $\acute{\varepsilon}$. Define

$$\hat{v} := \max_{\varepsilon \in \mathbf{E}_i - \{\acute{\varepsilon}\}} \left\{ d(\acute{O}, \varepsilon) \right\}, \qquad i \in \mathbf{n} \tag{17}$$

where $\mathbf{E}_i$ represents the set of all edges of polygon i, and suppose that the Minmax-edge circle is not tangent to any other edge, implying that $\delta = (\acute{r} - \hat{v})/2$ is positive. Let M be a point on $\acute{\varepsilon}$ or its extension, such that $M\acute{O} \perp \acute{\varepsilon}$. Let also $\hat{O}$ be a point on $M\acute{O}$ such that $\acute{O}\hat{O} = \delta$ (for example, see Fig. 6). According to Lemma 3, we have

$$d(\hat{O}, \varepsilon) \le d(\acute{O}, \varepsilon) + \delta \le \hat{v} + \delta \quad \forall \varepsilon \in \mathbf{E}_i - \{\acute{\varepsilon}\}. \tag{18}$$

From (18) and the relation $\hat{v} + \delta = \acute{r} - \delta < \acute{r}$, one can conclude that

$$\max_{\varepsilon \in \mathbf{E}_i} \left\{ d(\hat{O}, \varepsilon) \right\} < \acute{r} \quad i \in \mathbf{n} \tag{19}$$

which contradicts the fact that $\acute{O}$ is the Minmax-edge centroid. This completes the proof. ■

Lemma 5: The Minmax-edge circle of the ith Voronoi polygon is tangent to at least two edges. Furthermore, if the Minmax-edge circle is tangent to exactly two edges, say ε_1 and ε_2, then at least one of the following conditions holds.

1) The two edges ε_1 and ε_2 are parallel.
2) The centroid $\acute{O}_i$ is the intersection of the bisector of the angle between $\varepsilon_1, \varepsilon_2$, and one of the edges of the polygon.

Proof: Suppose the Minmax-edge circle is tangent to exactly two nonparallel Voronoi edges ε_1 and ε_2, but $\acute{O}$ is not the intersection of the bisector of the angle between ε_1 and ε_2 and an edge of the polygon; i.e., $\acute{O}$ is inside the polygon. Define

$$\tilde{v} := \max_{\varepsilon \in \mathbf{E}_i - \{\varepsilon_1, \varepsilon_2\}} \left\{ d(\acute{O}, \varepsilon) \right\} \quad i \in \mathbf{n}. \tag{20}$$

Since $C(\acute{O}, \acute{r})$ is tangent to exactly two edges, thus $\delta^* = (\acute{r} - \tilde{v})/2$ is positive. Let the point F be the intersection of ε_1 and ε_2 (or their extensions). Let also $\tilde{O}$ be a point on $F\acute{O}$ such that $\acute{O}\tilde{O} = \delta$, where δ is an arbitrary value in the interval $(0, \delta^*]$ (as an example, see Fig. 7). According to Lemma 3

$$d(\tilde{O}, \varepsilon) \leq d(\acute{O}, \varepsilon) + \delta \leq \tilde{v} + \delta, \quad \forall \varepsilon \in \mathbf{E}_i - \{\varepsilon_1, \varepsilon_2\}, \qquad i \in \mathbf{n}. \tag{21}$$

It results from (21) and the relations $\tilde{v} + \delta \leq \acute{r} - \delta < \acute{r}$ and $d(\tilde{O}, \varepsilon_1) = d(\tilde{O}, \varepsilon_2) < \acute{r}$ that

$$\max_{\varepsilon \in \mathbf{E}_i} \left\{ d(\tilde{O}, \varepsilon) \right\} < \acute{r}, \qquad i \in \mathbf{n} \tag{22}$$

which contradicts the fact that $\acute{O}$ is the Minmax-edge centroid. On the other hand, if the Minmax-edge circle is not touching exactly two Voronoi edges, then according to Lemma 4 it is tangent to at least three Voronoi edges. This completes the proof. ■

Lemma 6: If a Minmax-edge circle is tangent to two parallel edges, then there are generically other Minmax-edge circles as well, all of which are also tangent to these parallel edges.

Proof: Suppose one Minmax-edge circle, say C_1, is tangent to two parallel edges, say ε_1 and ε_2, but there exists another Minmax-edge circle, say C_2, that is not tangent to these two edges. Let the distance between ε_1 and ε_2 be denoted by $d(\varepsilon_1, \varepsilon_2)$. It is obvious that the radius of the circle C_1 is equal to $d(\varepsilon_1, \varepsilon_2)/2$. This implies that the radius of the circle C_2 must be grater than $d(\varepsilon_1, \varepsilon_2)/2$, which contradicts the initial assumption that C_2 is a Minmax-edge circle. ■

Remark 1: In the case when the Minmax-edge circles are tangent to two parallel edges, some of these circles are tangent to three or more edges. In this case, one of such circles is arbitrarily chosen as the Minmax-edge circle.

Definition 7: For convenience of notation, the circle touching two edges ε_g and ε_h of polygon i, centered at the intersection of the edge ε_k and the bisector of the angle between ε_g and ε_h is denoted by $\Omega^k_{g,h}$, for any $k, g, h \in \mathbf{e}_i := \{1, \ldots, e_i\}$, where e_i is the number of edges of polygon i in the Voronoi diagram.

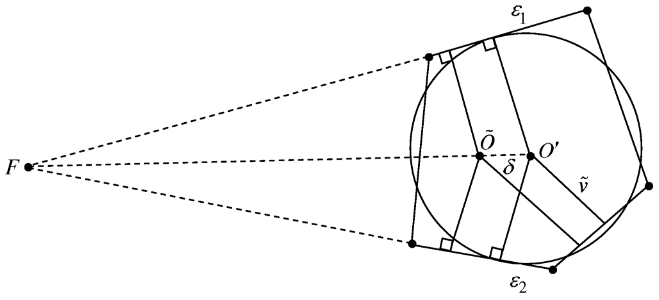

Fig. 7. Diagram used in the proof of Lemma 5.

Algorithm 2: Finding the Minmax-edge centroid of the i-th Voronoi polygon

```
begin
  1) for $f = 1,2,\ldots,e_i - 2$
       for $g = f+1, f+2, \ldots, e_i - 1$
         for $h = g+1, g+2, \ldots, e_i$
           calculate $\Omega^{f,g,h}$
           if $\Omega^{f,g,h}$ is centered inside or on the
           polygon and it intersects or is tangent to
           all edges of the polygon, then
               record it.
           end
         end
       end
     end
  2) for $g = 1,2,\ldots,e_i - 1$
       for $h = g+1, g+2, \ldots, e_i$
           calculate $\Omega^k_{g,h}$
           if $\Omega^{k,l}_{p,q}$ is centered inside or on the
           polygon and it intersects or is tangent to
           all edges of the polygon, then
               record it.
           end
       end
     end
  3) The center of the smallest circle is the
     Minmax-edge centroid of the polygon.
```

Also, the circle touching three edges ε_f, ε_g and ε_h of polygon i is denoted by $\Omega^{f,g,h}$, for $f, g, h \in \mathbf{e}_i$.

Theorem 3: Let $\breve{\mathbf{D}}_i$ be the set of all circles $\Omega^k_{g,h}, \forall k, g, h \in \mathbf{e}_i$, such that: 1) their centers lie inside or on the ith polygon and 2) they intersect or are tangent to all edges of the polygon. Let also $\grave{\mathbf{D}}_i$ be the set of all circles such that: 1) they are tangent to at least three edges of a Voronoi polygon; 2) their centers lie inside or on the ith polygon; and 3) they intersect or are tangent to all edges of the polygon. Define $\mathbf{D}_i := \breve{\mathbf{D}}_i \cup \grave{\mathbf{D}}_i$. Then, the Minmax-edge circle belongs to $\mathbf{D}_i$, and is the smallest circle in this set.

Proof: The proof follows directly from Lemmas 5 and 6, and Remark 1. ■

Using the result of Theorem 3, Algorithm 2 is developed to find the Minmax-edge centroid in the ith Voronoi polygon. The computational complexity of this algorithm is $O(e_i^4)$, which is typically not too high.

C. Maxmin-Edge Strategy

Similar to the two methods introduced so far, the idea behind this strategy is that when the sensors are evenly distributed, none

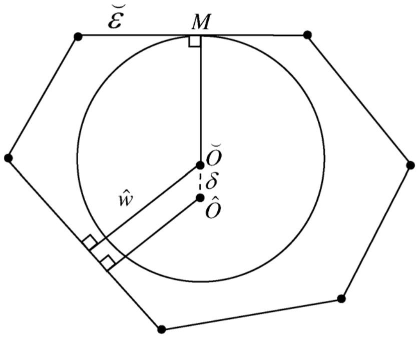

Fig. 8. Diagram used in the proof of Lemma 7.

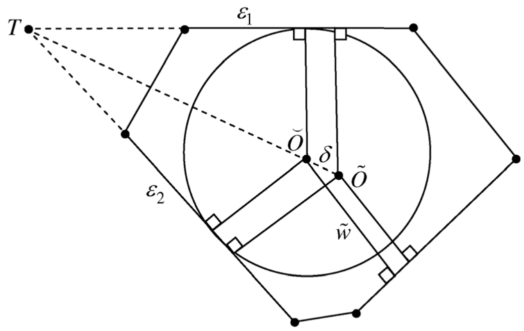

Fig. 9. Diagram used in the proof of Lemma 8.

of them should be too close to any of its Voronoi edges. The candidate location of a sensor under the Maxmin-edge strategy is a point inside the corresponding Voronoi polygon whose distance from the nearest Voronoi edge is the largest. This point will be referred to as the *Maxmin-edge centroid*, and will be denoted by $\breve{O}$. Furthermore, the distance between this point and the nearest edge to it will be represented by $\breve{r}$. The Maxmin-edge circle is defined next.

Definition 8: The Maxmin-edge circle of a polygon is the largest circle inside the polygon. This circle is, in fact, $C(\breve{O},\breve{r})$.

Lemma 7: The Maxmin-edge circle is tangent to at least two of the Voronoi edges.

Proof: Consider a Voronoi polygon, and let $\breve{\varepsilon}$ be the nearest edge to the Maxmin-edge centroid of the polygon. The radius $\breve{r}$ is equal to the distance between $\breve{O}$ and $\breve{\varepsilon}$, i.e. $\breve{r} = d(\breve{O},\breve{\varepsilon})$. Thus, $C(\breve{O},\breve{r})$ is tangent to $\breve{\varepsilon}$. Define

$$\hat{w} = \min_{\varepsilon\in\mathbf{E}_i-\{\breve{\varepsilon}\}} \left\{d(\breve{O},\varepsilon)\right\}, \qquad i\in\mathbf{n} \tag{23}$$

and suppose that the Maxmin-edge circle is not tangent to any other edge, implying that $\delta^* = (\breve{w}-\breve{r})/2$ is positive. Let M be a point on $\breve{\varepsilon}$, such that $M\breve{O} \perp \breve{\varepsilon}$. Let also $\hat{O}$ be a point on $M\breve{O}$ such that $\breve{O}\hat{O} = \delta$, where δ is an arbitrary value in the interval $(0,\delta^*]$ (as an example, see Fig. 8). According to Lemma 3, we have

$$d(\hat{O},\varepsilon) \ge d(\breve{O},\varepsilon) - \delta \ge \hat{w} - \delta, \quad \forall\varepsilon\in\mathbf{E}_i - \{\breve{\varepsilon}\}. \tag{24}$$

From (24) and the relation $\hat{w}-\delta \ge \breve{r}+\delta > \breve{r}$, one can conclude that

$$\min_{\varepsilon\in\mathbf{E}_i} \left\{d(\hat{O},\varepsilon)\right\} > \breve{r} \tag{25}$$

which contradicts the fact that $\breve{O}$ is the Maxmin-edge centroid. This completes the proof. ■

Lemma 8: If the Maxmin-edge circle is tangent to exactly two edges, then these two edges are parallel. Furthermore, in such a case there will generically be other Maxmin-edge circles, all of which are also tangent to these parallel edges.

Proof: Suppose a Maxmin-edge circle is tangent to exactly two Voronoi edges, say ε_1 and ε_2, but these two edges are not parallel. Let the point T be the intersection of ε_1 and ε_2 (or their extensions). Define

$$\tilde{w} := \min_{\varepsilon\in\mathbf{E}_i-\{\varepsilon_1,\varepsilon_2\}} \left\{d(\breve{O},\varepsilon)\right\}, \qquad i\in\mathbf{n}. \tag{26}$$

Since $C(\breve{O},\breve{r})$ is tangent to exactly two edges, the term $\delta^* = (\tilde{w}-\breve{r})/2$ is positive. Let also $\tilde{O}$ be a point on the extension of $T\breve{O}$ (closer to $\breve{O}$) such that $\breve{O}\tilde{O} = \delta$, where δ is an arbitrary value in the interval $(0,\delta^*]$ (as an example, see Fig. 9). According to Lemma 3, we have

$$\tilde{w}-\delta \le d(\breve{O},\varepsilon)-\delta \le d(\tilde{O},\varepsilon), \quad \forall\varepsilon\in\mathbf{E}_i-\{\varepsilon_1,\varepsilon_2\}, \qquad i\in\mathbf{n}. \tag{27}$$

It results from (27) and the relations $\breve{r} < \breve{r}+\delta \le \tilde{w}-\delta$ and $d(\tilde{O},\varepsilon_1) = d(\tilde{O},\varepsilon_2) > \breve{r}$ that

$$\min_{\varepsilon\in\mathbf{E}_i}\{d(\tilde{O},\varepsilon)\} > \breve{r}, \qquad i\in\mathbf{n} \tag{28}$$

which contradicts the fact that $\breve{O}$ is the Maxmin-edge centroid.

Now, suppose that one Maxmin-edge circle, say C_1, is tangent to two parallel edges, say ε_1 and ε_2, but there exists another Maxmin-edge circle, say C_2, that it is not tangent to these two edges. Note that the radius of the circle C_1 is equal to $d(\varepsilon_1,\varepsilon_2)/2$. This implies that the radius of the circle C_2 must be less than $d(\varepsilon_1,\varepsilon_2)/2$, which contradicts the initial assumption that C_2 is a Maxmin-edge circle. This completes the proof. ■

Remark 2: Similar to the Minmax-edge circle, in the case when the Maxmin-edge circles are tangent to two parallel edges, some of these circles are tangent to three or more edges. In this case, one of such circles is arbitrarily chosen as the Maxmin-edge circle.

Theorem 4: Let $\mathbf{Z}$ be the set of all circles which: 1) are tangent to at least three edges of a Voronoi polygon and 2) are inside the polygon. The Maxmin-edge circle belongs to $\mathbf{Z}$, and is the largest circle in this set.

Proof: According to Lemma 8 (and Remark 2), the Maxmin-edge circle is tangent to three or more Voronoi edges, and hence it is the incircle or excircle of the triangles created by these edges (possibly extended edges). It is known that $C(\breve{O},\breve{r}) \in \mathbf{Z}$; thus, it results from Definition 8 that $\breve{r} = \max_{C(O,r)\in\mathbf{Z}}\{r\}$. ■

According to Theorem 4, the Maxmin-edge centroid is the center of the incircle or excircle of one of the triangles created by

Algorithm 3: Finding the Maxmin-edge centroid of the i-th Voronoi polygon

```
begin
    1) for $f = 1, 2, \ldots, e_i - 2$
           for $g = f+1, f+2, \ldots, e_i - 1$
               for $h = g+1, g+2, \ldots, e_i$
                   calculate $\Omega^{f,g,h}$
                   if $\Omega^{f,g,h}$ is inside the polygon, then
                       record it.
                   end
               end
           end
       end
    2) The center of the largest circle is the
       Maxmin-edge centroid of the polygon.
```

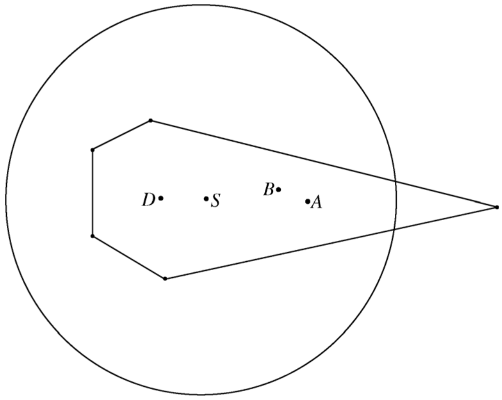

Fig. 10. Example of a configuration for which the edge-based strategies are not as effective.

three (extended) edges of the polygon. Hence, one can develop an algorithm of complexity $O(e_i^4)$ (which is typically not too high, as noted earlier) to find the Maxmin-edge centroid of a Voronoi polygon.

Remark 3: It is worth noting that one can also use a numerical approach such as linear programing or other existing techniques in order to find the centroid point of each region in the second phase of the proposed algorithms [34].

D. VEDGE Strategy

As noted earlier, sometimes the vertex-based algorithms are not suitable for coverage improvement, as illustrated in Fig. 4. On the other hand, in certain cases the vertex-based algorithms can outperform the edge-based ones in terms of coverage. For example, in Fig. 10 the candidate locations for sensor S using the VOR [13], Minimax [13], and Maxmin-edge strategies are the points A, B and D, respectively. It is clear in this case that the VOR and Minimax algorithms increase the coverage area, but the Maxmin-edge algorithm does not. This motivates the development of a new algorithm called VEDGE, as a combination of Minimax (as a vertex-based algorithm) and Maxmin-edge (as an edge-based algorithm). In each round of this algorithm, every sensor selects two points as its candidate locations: one point according to the Minimax strategy and the other one according to the Maxmin-edge strategy. Any of the two points that provides better coverage is selected as the new location of the sensor.

Remark 4: The problem investigated in this paper is a nonconvex optimization problem and all of the proposed algorithms are distributed. Thus, if every sensor moves to its optimal location in each iteration, it will not necessarily result in the optimal sensor configuration.

Remark 5: An important property of the Voronoi diagram is that it partitions the field in such a way that there is exactly one sensor in each Voronoi polygon. Since under the proposed algorithms the new candidate location of each sensor is inside its current Voronoi polygon, thus the sensor moves within its own Voronoi polygon only to reach the new location. This implies that the sensors will not collide. Assume now that there exists a sensor that cannot communicate with some of its neighbors, and consequently some of the edges of the resultant polygon may be different from those of the exact Voronoi polygon. As a result, the polygons constructed in this case do not necessarily partition the field in the sense that some of them may overlap with each other. This can have a negative impact on the detection of coverage holes. Furthermore, the overlap of the polygons can lead to sensor collisions.

Remark 6: In order to prevent oscillatory movement of the sensors, a control mechanism similar to the one in [13] is implemented. Under this mechanism, each sensor compares the newly computed direction with the previous one; it will not move in the current round if the new direction is backwards w.r.t. that in the preceding round.

IV. Simulation Results

Example 1: In this example, 30 sensors with the sensing range of 6 m and the communication range of 20 m are randomly deployed in a 50 m × 50 m flat surface. Fig. 11 depicts an operational example of the VEDGE strategy for the above setup. The algorithm is set to terminate when no sensor's coverage in its Voronoi polygon increases by more than 1% in its next move. Three snapshots are provided, and in each one both sensing circles of the sensors (filled circles) and the Voronoi diagram are depicted. After the first round of the algorithm, the coverage increases from the initial value of 60.7% to 81.7%. The algorithm terminates after 13 rounds, and the final coverage is 95.1%. It can be observed from this figure that in the final round the sensors are distributed more evenly than the initial configuration, resulting in significant increase in network coverage.

Remark 7: It is important to note that an analytical solution to the sensor deployment problem for optimal coverage is mathematically too complex to compute. This issue has also been pointed out in the literature, and the performance of any sensor deployment technique is typically evaluated by running a number of simulations with random initial positions for sensors [12], [13], [23], [31], [35], [36]. This approach will be adopted in the next example in order to evaluate the effectiveness of the proposed techniques.

Example 2: In this example, the proposed algorithms are applied to the same flat surface and the same type of sensor as the previous example. The results are then compared with the results of the algorithms given in [13]. In these simulations, the algorithms stop when none of the sensors' coverage in its Voronoi polygon would be improved by more than 1% in the next move. It is to be noted that all of the results presented in this example

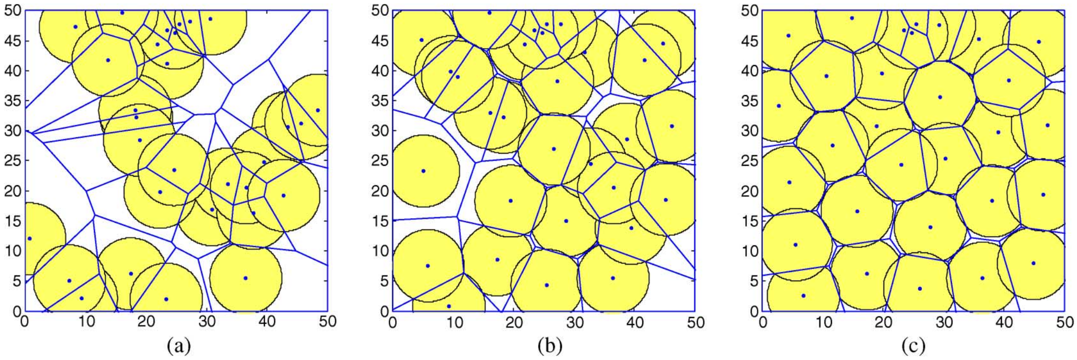

Fig. 11. Snapshots of the movement of sensors as well as the Voronoi polygons and sensing circles under the VEDGE strategy in Example 1. (a) Initial configuration of sensors. (b) Configuration of sensors after the first round. (c) Final configuration.

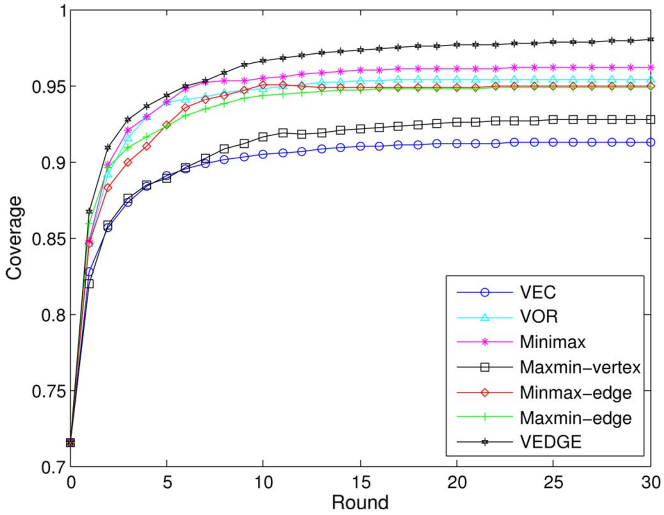

Fig. 12. The coverage factor for 30 sensors using different strategies.

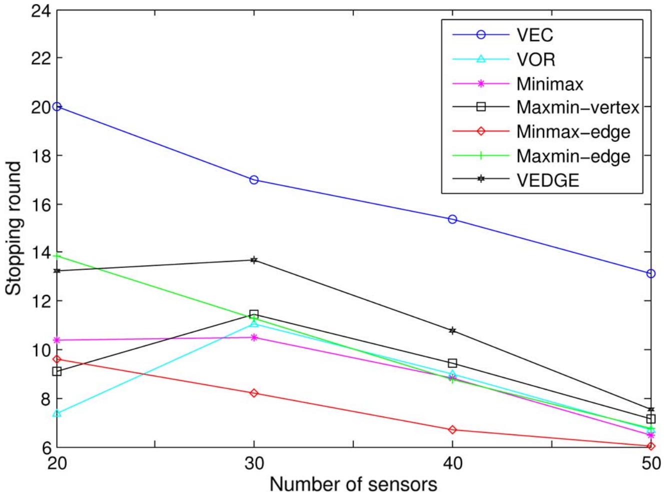

Fig. 13. Number of rounds required to reach the termination condition for different numbers of sensors using different strategies.

are the average values obtained by performing 100 simulations with random initial positions for sensors. Furthermore, while the horizontal axes of Figs. 13–16 represent a discrete quantity (number of sensors), the corresponding curves are depicted as continuous graphs for the sake of clarity.

Fig. 12 gives the coverage factor (the ratio of the covered area to the total area) for 30 sensors, calculated after each round of different algorithms. It can be observed that all algorithms reach a satisfactory coverage level in the first few rounds. The resultant curves also show that the VEDGE algorithm has the best coverage performance.

The time it takes for the network to reach the desired coverage level is another important criterion for measuring the efficiency of the algorithms. Since the deployment time of the sensors in each round is almost the same in all algorithms, the number of rounds required to reach a certain coverage level is used to evaluate time efficiency. Fig. 13 shows the stopping round of the algorithms for different number of sensors. The simulation is carried out for $n = 20, 30, 40, 50$. It can be seen from this figure that, for $n > 30$, the number of rounds decreases as the number of sensors increases. This is due to the fact that when the number of sensors is large, the probability that each sensor covers its Voronoi polygon becomes higher. As a result, the termination condition is satisfied in a shorter period of time in such cases. It can also be observed from Fig. 13 that the stopping round for the case of 20 sensors in the VOR strategy is less than that in the other strategies, but for 30 or more sensors the Minmax-edge algorithm converges faster.

Energy efficiency is another important measure of performance in mobile sensor networks. Energy consumption due to movement is known to be directly related to the moving distance of the sensors, as well as the number of times they stop (note that each time a sensor stops, it will need to overcome the static friction in the next movement). Thus, it is important to also compare the algorithms in terms of the overall moving distance of the sensors, and the number of times they stop. Fig. 14 depicts the average moving distance for different number of sensors using different algorithms. These graphs show that the average moving distance is smaller for a larger number of sensors (for the same reason given earlier). Simulations show that for small number of sensors, the Maxmin-vertex algorithm has the smallest average moving distance. The number of movements versus the number of sensors is given in Fig. 15. This figure shows that in most algorithms when the number of sensors increases from 20 to 30, the number of sensor movements also increases. The reason is that when there is a small number of sensors in the network, the Voronoi polygons are relatively

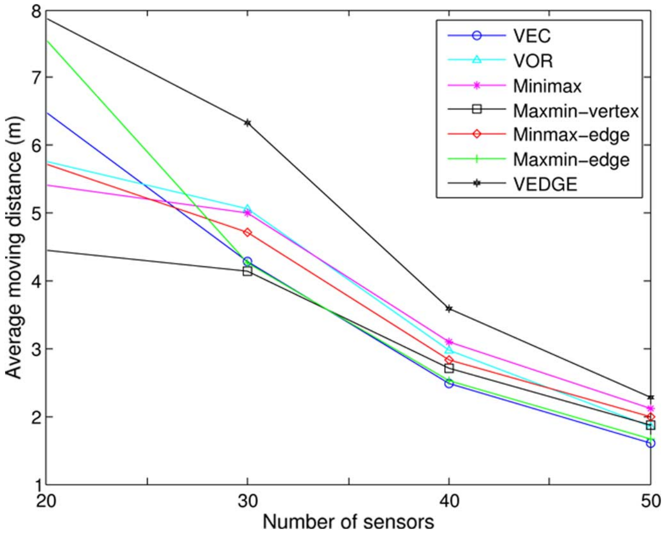

Fig. 14. Average distance each sensor travels for different number of sensors using different strategies.

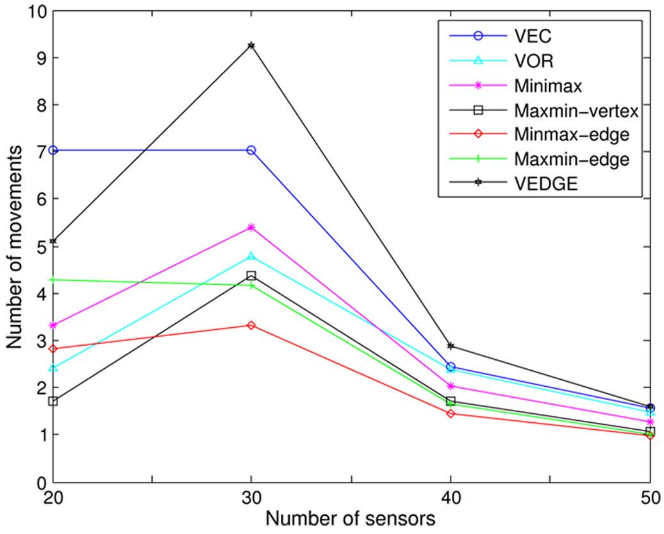

Fig. 15. Number of movements for different number of sensors using different strategies.

TABLE I
ENERGY CONSUMPTION IN JOULE FOR DIFFERENT NUMBER OF SENSORS USING DIFFERENT ALGORITHMS

	$n = 20$	$n = 30$	$n = 40$	$n = 50$
VEC	111.5994 J	93.6881 J	40.7438 J	26.2542 J
VOR	67.4912 J	81.3886 J	44.3346 J	27.59789 J
Minimax	72.1187 J	86.0919 J	42.3478 J	27.9395 J
Maxmin-vertx	58.9354 J	77.4206 J	39.5842 J	26.3091 J
Minmax-edge	70.5660 J	66.4283 J	35.2764 J	24.5355 J
Maxmin-edge	97.7894 J	69.7719 J	34.5885 J	22.1933 J
VEDGE	107.3883 J	128.8364 J	53.4931 J	31.8599 J

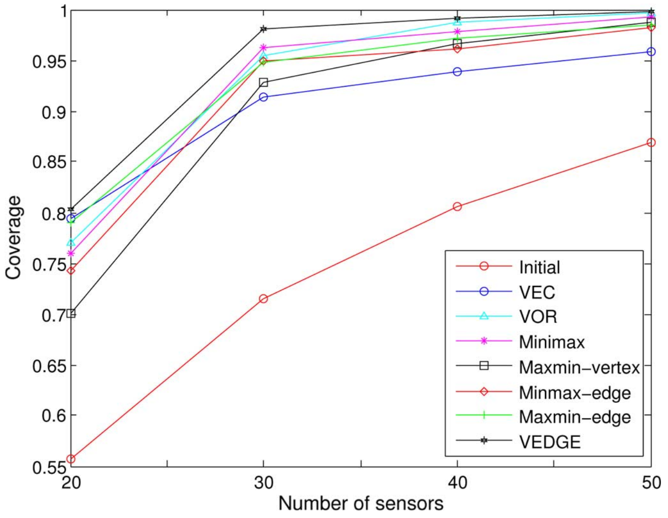

Fig. 16. Coverage factor for different number of sensors using different strategies.

large compared to the sensing circles. Thus, it is likely that each Voronoi polygon completely contains the sensing circle of the sensor inside it. This implies that the sensor's local coverage is maximum (i.e., it is equal to the area of the sensing circle), and hence it will likely not increase if the sensor moves in any direction. However, when the number of sensors increases beyond 30, then the number of movements decreases considerably. In fact, when the number of sensors increases beyond a certain value, it is more likely that each sensor covers its Voronoi polygon. Hence, the termination condition will be satisfied in a shorter period of time, resulting in a decrease in the number of movements. Fig. 15 confirms this expectation and shows that, as the number of sensors increases beyond 30, the number of required movements decreases.

Assume that the energy required to move a sensor a 1-m distance (without stopping in between) is 8.268J [33], [37]. Let the energy required to stop a sensor and then overcome the static friction (in order to move it) be also equal to the above value [23]. Table I summarizes the results, where it can be observed that when the number of sensors in the network is not large, the Maxmin-vertex strategy outperforms the other techniques in terms of energy consumption. For a large number of sensors, on the other hand, the Maxmin-edge strategy is more energy-efficient compared to the other methods.

In Fig. 16, the final coverage of each strategy is depicted for different number of sensors. It can be observed that the VEDGE algorithm has the largest final coverage in all scenarios. It is also interesting to note that although the VEC algorithm does not have a good performance for large number of sensors, it performs relatively well for small number of sensors.

It follows from the above discussion that the choice of an appropriate deployment algorithm involves a trade-off between three main factors: network coverage, deployment time, and energy efficiency. The discussion is summarized below.

1) The VEDGE algorithm outperforms the other algorithms as far as network coverage is concerned.
2) The Minmax-edge algorithm is more desirable when the deployment time is the main concern AND the number of sensors in the field is not small.
3) The Maxmin-vertex algorithm is more preferable when the energy consumption is the main concern AND the number of sensors in the field is not large.
4) The Maxmin-edge algorithm is more energy-efficient than the other algorithms when there is a large number of sensors in the network.

V. Conclusion

Distributed sensor deployment strategies are proposed in this work for efficient field coverage in a mobile sensor network. Under these strategies, each sensor moves iteratively in a direction that the coverage holes in its Voronoi polygon are reduced. The proposed strategies tend to place the sensors in such a way that undesirable network configurations are avoided. The Maxmin-vertex strategy selects each sensor's candidate location as a point inside its Voronoi polygon whose distance from the nearest Voronoi vertex is the largest. The Minmax-edge strategy, on the other hand, selects the candidate location as a point inside its Voronoi polygon whose distance from the farthest Voronoi edge is the smallest. The Maxmin-edge strategy selects the candidate location as a point inside its Voronoi polygon whose distance from the nearest Voronoi edge is the largest. Finally, the VEDGE strategy is a combination of the Minimax algorithm (introduced in the literature) and Maxmin-edge algorithm. Two candidate points are calculated for each sensor based on these two methods, and the one which provides better coverage is selected as the candidate location for that sensor. In all of these techniques, each sensor moves to the new location only if its coverage increases. Simulations demonstrate the advantages of the proposed techniques compared with other known methods.

Acknowledgment

The authors would like to thank W. Masoudimansour for helpful discussions and suggestions.

References

[1] A. Koubaa, R. Severino, M. Alves, and E. Tovar, "Improving quality-of-service in wireless sensor networks by mitigating hidden-node collisions," *IEEE Trans. Ind. Inf.*, vol. 5, no. 3, pp. 299–313, Aug. 2009.

[2] S. Martinez, "Distributed interpolation schemes for field estimation by mobile sensor networks," *IEEE Trans. Control Syst. Technol.*, vol. 18, no. 2, pp. 491–500, Feb. 2010.

[3] Y.-C. Wang, W.-C. Peng, and Y.-C. Tseng, "Energy-balanced dispatch of mobile sensors in a hybrid wireless sensor network," *IEEE Trans. Parallel Distrib. Syst.*, vol. 21, no. 12, pp. 1836–1850, Dec. 2010.

[4] J. Haase, J. Molina, and D. Dietrich, "Power-aware system design of wireless sensor networks: Power estimation and power profiling strategies," *IEEE Trans. Ind. Inf.*, vol. 7, no. 4, pp. 601–613, Nov. 2011.

[5] O. Omeni, A. C. W. Wong, A. J. Burdett, and C. Toumazou, "Energy efficient medium access protocol for wireless medical body area sensor networks," *IEEE Trans. Biomed. Circuits Syst.*, vol. 2, no. 4, pp. 251–259, Dec. 2008.

[6] H. Mahboubi, A. Momeni, A. G. Aghdam, K. Sayrafian-Pour, and V. Marbukh, "An efficient target monitoring scheme with controlled node mobility for sensor networks," *IEEE Trans. Control Syst. Technol.*, vol. 20, no. 6, pp. 1522–1532, Jun. 2012.

[7] X. Chang, R. Tan, G. Xing, Z. Yuan, C. Lu, Y. Chen, and Y. Yang, "Sensor placement algorithms for fusion-based surveillance networks," *IEEE Trans. Parallel Distrib. Syst.*, vol. 22, no. 8, pp. 1407–1414, Aug. 2011.

[8] J. Lu and T. Suda, "Differentiated surveillance for static and random mobile sensor networks," *IEEE Trans. Wireless Commun.*, vol. 7, no. 11, pp. 4411–4423, Nov. 2008.

[9] T. Clouqueur, V. Phipatanasuphorn, P. Ramanathan, and K. K. Saluja, "Sensor deployment strategy for target detection," in *Proc. 1st ACM Int. Workshop on Wireless Sensor Networks and Applications*, 2002, pp. 42–48.

[10] G. Anastasi, M. Conti, and M. Di Francesco, "Extending the lifetime of wireless sensor networks through adaptive sleep," *IEEE Trans. Ind. Inf.*, vol. 5, no. 3, pp. 351–365, Aug. 2009.

[11] L. Lobello and E. Toscano, "An adaptive approach to topology management in large and dense real-time wireless sensor networks," *IEEE Trans. Ind. Inf.*, vol. 5, no. 3, pp. 314–324, Aug. 2009.

[12] A. Howard, M. J. Matarić, and G. S. Sukhatme, "An incremental self-deployment algorithm for mobile sensor networks," *Autonomous Robots*, vol. 13, no. 2, pp. 113–126, 2002.

[13] G. Wang, G. Cao, and T. F. L. Porta, "Movement-assisted sensor deployment," *IEEE Trans. Mobile Computing*, vol. 5, no. 6, pp. 640–652, 2006.

[14] D. Wang, J. Liu, and Q. Zhang, "Mobility-assisted sensor networking for field coverage," in *Proc. IEEE Global Commun. Conf.*, 2007, pp. 1190–1194.

[15] J. Cortes, S. Martinez, and F. Bullo, "Spatially-distributed coverage optimization and control with limited-range interactions," *ESAIM. Control, Optimisation and Calculus of Variations*, vol. 11, pp. 691–719, 2005.

[16] H. Mahboubi, K. Moezzi, A. G. Aghdam, K. Sayrafian-Pour, and V. Marbukh, "Self-deployment algorithms for coverage problem in a network of mobile sensors with unidentical sensing range," in *Proc. IEEE Global Commun. Conf.*, 2010, pp. 1–6.

[17] X. Li, A. Nayak, and I. Stojmenovic, *Wireless Sensor and Actuator Networks: Algorithms and Protocols for Scalable Coordination and Data Communication*. New York, NY, USA: Wiley-Interscience, 2010.

[18] M.-C. Zhao, J. Lei, M.-Y. Wu, Y. Liu, and W. Shu, "Surface coverage in wireless sensor networks," in *Pro. 28th IEEE INFOCOM*, 2009, pp. 109–117.

[19] M. Pavone, E. Frazzoli, and F. Bullo, "Distributed policies for equitable partitioning: Theory and applications," in *Proc. 47th IEEE Conf. Decision and Control*, 2008, pp. 4191–4197.

[20] J. Cortes and F. Bullo, "Coordination and geometric optimization via distributed dynamical systems," *SIAM J. Control and Optimization*, vol. 44, no. 5, pp. 1543–1574, 2006.

[21] S. Susca, F. Bullo, and S. Martinez, "Monitoring environmental boundaries with a robotic sensor network," *IEEE Trans. Control Syst. Technol.*, vol. 16, no. 2, pp. 288–296, Feb. 2008.

[22] J.-W. Lee, B.-S. Choi, and J.-J. Lee, "Energy-efficient coverage of wireless sensor networks using ant colony optimization with three types of pheromones," *IEEE Trans. Ind. Inf.*, vol. 7, no. 3, pp. 419–427, Aug. 2011.

[23] G. Wang, G. Cao, P. Berman, and T. F. L. Porta, "A bidding protocol for deploying mobile sensors," *IEEE Trans. Mobile Computing*, vol. 6, no. 5, pp. 563–576, 2007.

[24] Q. Du, V. Faber, and M. Gunzburger, "Centroidal Voronoi tessellations: Applications and algorithms," *SIAM Rev.*, vol. 41, pp. 637–676, 1999.

[25] R. Klein, *Concrete and Abstract Voronoi Diagrams*. Berlin, Germany: Springer, 1989.

[26] H. Mahboubi, J. Habibi, A. G. Aghdam, and K. Sayrafian-Pour, "Distributed deployment strategies for improved coverage in a network of mobile sensors with prioritized sensing field," *IEEE Trans. Ind. Inf.*, vol. 9, no. 1, pp. 451–461, Feb. 2013.

[27] D. E. Koditschek, *Robot Planning and Control Via Potential Functions*. Cambridge, MA, USA: MIT, 1989.

[28] H. Mahboubi, K. Moezzi, A. G. Aghdam, K. Sayrafian-Pour, and V. Marbukh, "Distributed deployment algorithms for improved coverage in mobile sensor networks," in *Proc. IEEE Multiconf. Syst. and Control*, 2011, pp. 1244–1249.

[29] D. Niculescu and B. Nath, "Ad hoc positioning system (APS) using AOA," in *Proc. 22nd IEEE INFOCOM*, 2003, pp. 1734–1743.

[30] C. Intanagonwiwat, R. Govindan, and D. Estrin, "Directed diffusion: A scalable and robust communication paradigm for sensor networks," in *Proc. 6th Annu. Int. Conf. Mobile Computing and Networking*, 2000, pp. 56–67.

[31] A. Kwok and S. Martinez, "A distributed deterministic annealing algorithm for limited-range sensor coverage," *IEEE Trans. Control Syst. Technol.*, vol. 19, no. 4, pp. 792–804, Nov. 2011.

[32] Y.-C. Wang and Y.-C. Tseng, "Distributed deployment schemes for mobile wireless sensor networks to ensure multilevel coverage," *IEEE Trans. Parallel Distrib. Syst.*, vol. 19, no. 9, pp. 1280–1294, Sep. 2008.

[33] S. Yoon, O. Soysal, M. Demirbas, and C. Qiao, "Coordinated locomotion and monitoring using autonomous mobile sensor nodes," *IEEE Trans. Parallel Distrib. Syst.*, vol. 22, no. 10, pp. 1742–1756, Oct. 2011.

[34] S. P. Boyd and L. Vandenberghe, *Convex Optimization*. Cambridge, MA, USA: Cambridge Univ., 2004.

[35] J. Luo, D. Wang, and Q. Zhang, "On the double mobility problem for water surface coverage with mobile sensor networks," *IEEE Trans. Parallel Distrib. Syst.*, vol. 23, no. 1, pp. 146–159, 2012.

[36] X. Li, H. Frey, N. Santoro, and I. Stojmenovic, "Strictly localized sensor self-deployment for optimal focused coverage," *IEEE Trans. Mobile Computing*, vol. 10, no. 11, pp. 1520–1533, 2011.

[37] M. Rahimi, H. Shah, G. S. Sukhatme, J. Heideman, and D. Estrin, "Studying the feasibility of energy harvesting in a mobile sensor network," in *Proc. IEEE Int. Conf. Robot. Autom.*, 2003, vol. 1, pp. 19–24.

Hamid Mahboubi (M'13) received the B.Sc. degree in electrical engineering from Sharif University of Technology, Tehran, Iran, in 2003, and the M.A.Sc. degree in electrical and computer engineering from the University of Tehran, Tehran, Iran, in 2006. He is currently working toward the Ph.D. degree at the Department of Electrical and Computer Engineering, Concordia University, Montreal, QC, Canada.

His research interests include mobile sensor networks, multi-agent systems, hybrid systems, and optimization.

Mr. Mahboubi is the recipient of Fonds québécois de la recherche sur la nature et les technologies (FQRNT) Post-Doctoral Award, Bourse d'Etudes Hydro Quebec Scholarship, Power Corporation of Canada Graduate Fellowship, Canadian National Award in Transportation, and Concordia University Graduate Fellowship. He was a recipient of the Gold Medal in the 1999 National Math Olympiad in Iran. He has served as Chair of the Control Systems Chapter of the IEEE Montreal Section since January 2012.

Kaveh Moezzi (M'11) received the B.Sc. and M.Sc. degrees in electrical engineering from Amirkabir University of Technology (Tehran Polytechnic), Tehran, Iran, in 2002 and 2005, respectively, and the Ph.D. degree from Concordia University, Montreal, QC, Canada, in 2010.

He is currently a Systems Engineer with AKKA Technologies, Montreal, QC, Canada. His research interests include adaptive control, time-delay systems and robotics.

Dr. Moezzi was Control Systems Chapter Chair of the IEEE Montreal Section in 2010, when it was recognized as the most active chapter of the IEEE Control Systems Society.

Amir G. Aghdam (SM'05) received the B.A.Sc. degree in electrical engineering from Isfahan University of Technology, Isfahan, Iran, the M.A.Sc. degree in electrical engineering from Sharif University of Technology, Tehran, Iran, and the Ph.D. degree from the University of Toronto, Toronto, ON, Canada, in 2000.

He was a Development Engineer with Voyan Technology, Santa Clara, CA, USA, from 2000 to 2001. He was a Postdoctoral Researcher with the Systems Control Group of the University of Toronto, Toronto, ON, Canada, for six months and then joined Concordia University, Montreal, QC, Canada, in 2002, where he is currently a Professor with the Department of Electrical and Computer Engineering. His research interests include decentralized control of large-scale systems, multi-agent systems, switching control, and sampled-data systems.

Dr. Aghdam is a member of Professional Engineers of Ontario. He served as Chair of the IEEE Montreal Section and Chair of the Control Systems Chapter of the IEEE Montreal Section (2005–2006) and Chair of the IEEE Eastern Canada Area (2007–2009). He was the Editor-in-Chief of *IEEE Canadian Review* (2010–2012) and General Chair of the 2012 IEEE Canadian Conference on Electrical and Computer Engineering. He is a member of the Conference Editorial Board of the IEEE Control Systems Society, Co-Editor-in-Chief of the IEEE SYSTEMS JOURNAL, an associate editor of the IEEE TRANSACTIONS ON CONTROL SYSTEMS TECHNOLOGY, and *European Journal of Control*. He has been a Technical Program Committee Member of a number conferences including the IEEE Conference on Control Applications, the IEEE Conference on Decision and Control, and the American Control Conference. Since August 2013, he has been a member of Natural Sciences and Engineering Research Council of Canada (NSERC) ECE Evaluation Group. He was a recipient of the 2009 IEEE MGA Achievement Award and 2011 IEEE Canada J. J. Archambault Eastern Canada Merit Award.

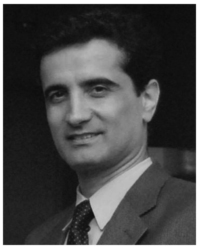

Kamran Sayrafian-Pour (SM'05) holds Ph.D., M.S. and B.S. degrees in Electrical & Computer Engineering from University of Maryland, Villanova University and Sharif University of Technology, respectively. He is currently a program lead at the Information Technology Laboratory of the National Institute of Standards and Technology (NIST) located in Gaithersburg, Maryland. Prior to this, he was the cofounder of Zagros Networks, Inc. a fabless semiconductor company based in Rockville, Maryland where he served as President and senior member of the architecture team. Dr. Sayrafian-Pour has been an adjunct faculty of the University of Maryland since 2003. He has served as an invited member of the technical program committee of many international conferences. He has also been the co-chair and organizer of several IEEE ComSoc Conferences and workshops focused on application of wireless communication in healthcare. His research interests include medical body area networks, mobile sensor networks and RF-based indoor positioning. He has published over 100 conference and journal papers, and book chapters in these areas. He was the recipient of the IEEE PIMRC 2009 & SENSORCOMM 2011 best paper awards, and has been a Guest Editor for a number of special issues focusing on the pervasive healthcare technologies and sensor networks. Dr. Sayrafian-Pour is a member of the COST Action IC1004 "Cooperative Radio Communications for Green Smart Environments; and, his research results have been included in the final report of the COST Action 2100 (Pervasive Mobile and Ambient Wireless Communications), which was published by Springer in January 2012. He was also a contributing member and the co-editor of the channel modeling document of the IEEE802.15.6 international standardization on body area networks. He is the co-inventor/inventor of four U.S. patents.

Vladimir Marbukh (M'99–SM'02) received the M.S. and Ph.D. degrees in applied mathematics from Saint Petersburg Technical University, Saint Petersburg, Russia, in 1973 and 1986, respectively.

He was with the Faculty of the Industrial Academy, Saint Petersburg, Russia, until 1988, and then in 1989 he moved to the U.S. and became a consultant to the Mathematics Department of AT&T Bell Laboratories, Murray Hill, NJ, USA. Since 1998, he has been with the National Institute of Standards and Technology (NIST), Gaithersburg, MD, USA, first in the Advanced Networking Technologies and then in the Computational and Applied Mathematics Division. His research interests include performance analysis and optimization of communication network using Operations Research, stochastic processes, and game theory.